Assessing the Importance of V(IV) During NH3-SCR Using Operando EPR Spectroscopy

Godiksen, Anita Lundager; Funk, Marie H.; Rasmussen, Søren Birk; Mossin, Susanne

Published in:
ChemCatChem

Link to article, DOI:
10.1002/cctc.202000802

Publication date:
2020

Document Version
Peer reviewed version

FULL PAPER

Assessing the Importance of V(IV) During NH_3-SCR Using *Operando* EPR Spectroscopy

Anita L. Godiksen[b], Marie H. Funk[a], Søren B. Rasmussen*[b], Susanne Mossin*[a]

Abstract: Suggested mechanisms for NH_3-SCR on V_2O_5/TiO_2 based catalysts contain both oxidized and reduced vanadium species. The degree of reduction and the importance of the redox properties of the catalyst are however still widely discussed. Here we show the presence of significant amounts of oxidovanadium(IV), VO^{2+} using electron paramagnetic resonance (EPR) spectroscopy of V_2O_5/TiO_2 and $V_2O_5/WO_3/TiO_2$ under *operando* selective catalytic reduction (SCR) of NO with NH_3 in a fixed bed plug flow reactor operating at high space velocity: 420,000 h^{-1}. The V(IV) content at the completely oxidized and reduced states is also analyzed. It is found that a significant part of the vanadium is reduced to the EPR active species, VO^{2+} at *operando* SCR conditions and even more when O_2 is removed from the SCR gas.

Introduction

The selective catalytic reduction of NO_x by ammonia (NH_3-SCR) with titania supported vanadium oxide catalysts is widely used commercially. Titania exhibits the appropriate interaction with surface vanadia species and is very robust in industrial off gas treatment in the temperature range 200-450°C. Especially the sulfur dioxide resistance and the performance compared to production price is outstanding, which ensures that vanadium-based catalysts will continue to play a major role industrially.

Vanadia dispersed over a titania (anatase) carrier is present as isolated or polymerized oxido and hydroxido vanadium(V) species when the total surface density of vanadium is less than around 8 V atoms pr. nm^2. Above this limit, often referred to as the monolayer capacity, nanocrystalline V_2O_5 starts to build up on the catalyst in addition to the dispersed species. At temperatures above 200°C, the SCR reaction behaves according to an Eley-Rideal type mechanism[1–9]. NH_3 is present as adsorbed species on the surface whereas NO reacts practically directly from the gas phase.

Raman and Fourier Transform Infrared (FTIR) spectroscopy have proven to be valuable methods for establishing the surface chemistry of vanadia at near SCR relevant conditions. FTIR spectroscopy has demonstrated the existence of a complicated ensemble of functional groups on the surface such as V-OH, W-OH, Ti-OH, V=O, adsorbed NH_3 and NH_4^+.[7] The distribution depends on the surface density of the transition metal oxide species and on the gas phase composition. Raman spectroscopy clearly identify oxide phases present in the bulk (TiO_2) and surface V-O_X and W-O_X of the catalyst.[3] Neither of these methods are directly sensitive to the oxidation state of vanadium. EPR spectroscopy is complimentary to these methods since it can only detect certain paramagnetic V(IV) species whereas V(V) is diamagnetic and therefore EPR silent. It is possible to set up a reactor heated with a flow of gas within the cavity of the EPR instrument and perform *operando* studies of the SCR reaction. Valuable information has thus been obtained by EPR spectroscopy on catalytic systems either *ex-situ* after activation at relevant conditions[10–12] or *operando* and *in-situ* at high temperatures: This includes investigations of V(IV), Cu(II) and Fe(III).[13–16]

Vanadium(V) is found as oxidovanadium(V) (VO^{3+}) in both isolated and polymeric species on the surface of the anatase support. At low vanadia loadings isolated vanadium(V) species are dominant and have in general been considered to be four coordinate with three V-O-Ti bonds in addition to the apical oxido group. Some studies have pointed out that during *operando* SCR the water content is sufficient to hydrolyze one of the V-O-Ti bonds,[3,9,17] so that the most abundant isolated vanadium(V) species on the surface at the reaction conditions contain at least one OH group. As the coverage increases at higher vanadia loadings, the condensation of V-OH species becomes extensive and V-O-V bonds are formed.

Vanadium(IV) is commonly found in the form of oxidovanadium(IV) (VO^{2+}, vanadyl) which is known to be stable under a wide range of conditions and environments. Oxidovanadium(IV) species are usually tetragonal with 4 ligands in a plane perpendicular to the apical V=O bond. Often a more distant sixth donor is also present trans to the oxido group resulting in 6-coordination. The energetically well-separated ground state of tetragonal 5- or 6-coordinate oxidovanadium(IV) species results in a distinct EPR signal with hyperfine coupling to the ^{51}V nuclei (I = 7/2, 100 % abundance). The EPR signal can be observed at temperatures relevant for the SCR reaction due to slow relaxation of the excited spin state and it has earlier been used by J. Due-Hansen et al. in combination with UV-vis spectroscopy to identify the interplay between the V(III), V(IV) and V(V) redox states during exposure of V_2O_5/TiO_2 catalysts to hydrogen-oxygen mixtures[18]. Later, the UV-vis results were confirmed by I. Wachs et al., discussing the presence of V(IV) sites in relation to surface intermediates during SCR[19,20].

Though Raman spectroscopy is not as sensitive to V(IV)=O species as EPR spectroscopy, careful analysis has revealed that at least part of the vanadium that is reduced at SCR conditions retains its V=O entity. This has also been shown by DFT calculations[21,22]. The relevance of vanadyl(IV) makes EPR spectroscopy a highly relevant tool for further analysis of the reduced vanadium species.

Non-oxido V(IV) is normally considered unstable under ambient or high temperatures or with access to water. Under a protective atmosphere or using specialized ligands, however, non-oxido coordination compounds of V(IV) may be isolated and characterized.[23] Under reducing conditions vanadium(III) and

[a] M.Sc. Marie H. Funk, Assoc. Prof. Susanne Mossin
Centre for Catalysis and Sustainable Chemistry, DTU Chemistry, Technical University of Denmark
Kemitorvet 207, 2800 Kgs. Lyngby, Denmark
E-mail: slmo@kemi.dtu.dk

[b] Ph.D. Søren B. Rasmussen, Ph.D. Anita L. Godiksen
Haldor Topsøe A/S
Haldor Topsøe Alle 1, 2800 Kgs. Lyngby, Denmark
E-mail: sobr@topsoe.com

Supporting information for this article is given via a link at the end of the document.

vanadium(II) compounds can also be isolated. Due to the high reactivity and strong reducing nature of V(III) and V(II) these oxidation states are not expected to be relevant in the presence of oxygen and water.

In this manuscript we argue that all vanadium species present in the surface layer during exposure to NO and O_2 is oxidovanadium(V) species and that EPR provides positive evidence for tetragonal oxidovanadium(IV) species being present in significant amounts under *operando* SCR and in even higher amounts after *in-situ* exposure to NO and NH_3. We use EPR to analyse the amount of tetragonal oxidovanadium(IV) present in the material during SCR and monitor both oxidation and reduction of the catalyst by changing the gas composition.

The mechanism for the SCR process and the role of vanadium (IV) species are still under debate[1,2,22,24–26]. The observation by EPR presented here show that a significant percentage of tetragonal oxidovanadium(IV) species is present under reaction conditions which is in accordance with the suggested mechanism presented by Arnason et al.[27]

Results and Discussion

Four samples with varying vanadium and tungsten loading are analysed in this study. The content of V and W determined by ICP and the BET surface area of the four investigated samples are given in Table 1. The IR and Raman spectra of the samples after activation in air flow at 400 °C are found in Figure 1 and Figure 2. The samples are comparable to similar $V_2O_5/WO_3/TiO_2$ samples, with the V3 samples having approximately half a monolayer coverage (around 3.9 V/nm^2) and the V6 samples a full monolayer coverage (7.8 V/nm^2). The FTIR spectra of the V3 samples show the V-OH stretching band at around 3655 cm^{-1}. In accordance with the literature, the band shifts to lower wavenumbers with increasing V load as a result of the polymeric nature of the V species at higher loadings[7]. The increase in intensity of the V=O overtone band with increasing vanadium loading is observed in Figure 1 b). The Raman spectra show the characteristic TiO_2 E_g band 640 cm^{-1}[28]. From the inset it is seen that the samples contain both monomeric and polymeric vanadium species. The bands at 1031-1035 cm^{-1} are assigned to the V=O stretching mode of predominantly isolated distorted tetrahedral monovanadates. The broad band at 900-950 cm^{-1} arises from the V-O stretching modes, primarily polyvanadate V-O-V modes[29–31]. The sharp band at 992 cm^{-1} is due to crystalline V_2O_5 on the anatase surface and indicates a high vanadium loading on the V6W3 sample exceeding the monolayer coverage. The band at 800 cm^{-1} is an overtone vibration of the anatase support which is stronger for the lower V loading catalysts[32].

Table 1. ICP determined composition along with their BET surface area.

	Content from ICP			BET surface area
	w%			
	V_2O_5	V	WO_3	m^2/g
V3W3	3.24	1.81	4.29	55
V6W3	6.09	3.41	3.41	44
V6W0	5.66	3.17	0.26	50
V3W0	3.42	1.92	0.12	59

The results from the EPR investigation of the V3W3 sample during SCR with and without O_2 are shown as absorption spectra (the first integral of the measured first-derivative EPR spectra) in Figure 3. It is obvious that the EPR signal intensity increases upon removal of O_2 from the feed gas and decreases again to the same level upon reintroduction of O_2. Some broadening of the spectra was observed upon removing O_2 (see Figure S1). The first and subsequent cycles gave identical results showing the stability of the used *in-situ* setup and the reproducibility of the experiments.

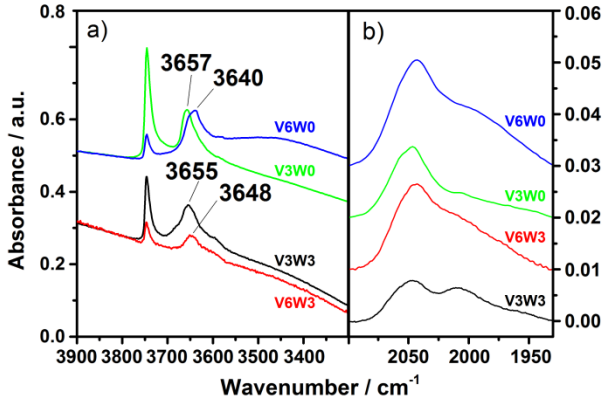

Figure 1. IR spectra of the $V_2O_5/WO_3/TiO_2$ samples. a) the V-OH stretching band area. b) the V=O overtone band.

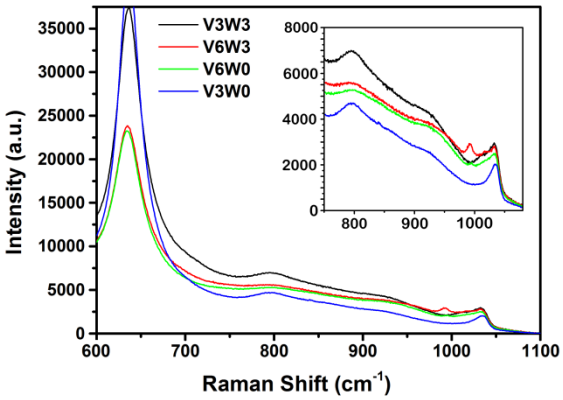

Figure 2. Raman spectra of the $V_2O_5/WO_3/TiO_2$ samples recorded at 80 ˚C after activation in air flow at 400 ˚C.

In Figure 4, top, the same data are given as EPR signal intensity (the double integral of the EPR spectra) and have been referenced to the total vanadium content using spectra of

oxidovanadium(IV) reference samples. In order to assess whether the experiments were run during actual *operando* conditions the exhaust gas composition was monitored continuously throughout the experiment and this is plotted on the same time scale, see Figure 4 bottom for the result for V3W3. The EPR signal intensity along with the exhaust gas composition for all samples are shown in Figure S2 and S3 at 250 °C and 200 °C, respectively. The NO conversion was found to be 80 – 85 % at 250 °C and 35 – 40 % at 200 °C for all 4 catalysts under *operando* SCR and was approximately zero for all samples under NO + NH_3 after the steady state was reached. This confirms that measurements were conducted during the actual working conditions for the catalysts.

The samples were also tested in a cycle from fully reducing (NO + NH_3) to fully oxidizing conditions (NO + O_2) at 250 °C in a separate experiment. The development of the EPR signal intensity for V3W3 is shown in Figure 5. The corresponding data for all samples and selected EPR spectra are given in Figure S4 and S5, respectively. To assess the spectra of the catalyst in the fully oxidized state, spectra were measured under O_2 alone and under NO + O_2 combined. These two spectra are compared in Figure 5, left and are found to be identical. (See Figures S6 and S7 for data for all samples)

For completeness, a control experiment was performed to investigate if any nitrates present would induce a change in the spectra, which had previously been observed on EPR of Cu-SSZ-13[33,34]: V3W3 was exposed first to a flow of NO + O_2 and then to a flow of NO (see Figure S8). The change in both intensity and spectrum were negligible. This control experiment was only performed on the V3W3 sample, since this sample was previously seen to give the strongest response to changes in the gas flows.

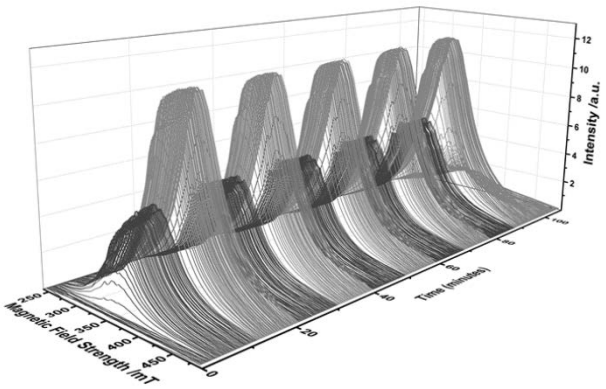

Figure 3. Stacked plot of the background corrected EPR absorption spectra obtained on the V3W3 sample through alternating between standard *operando* SCR (NH_3 + NO + O_2, dark grey) and *in-situ* under NH_3 + NO (light grey) at 250 °C. The time resolution is 4 spectra/min, the gas composition was switched every 10 minutes

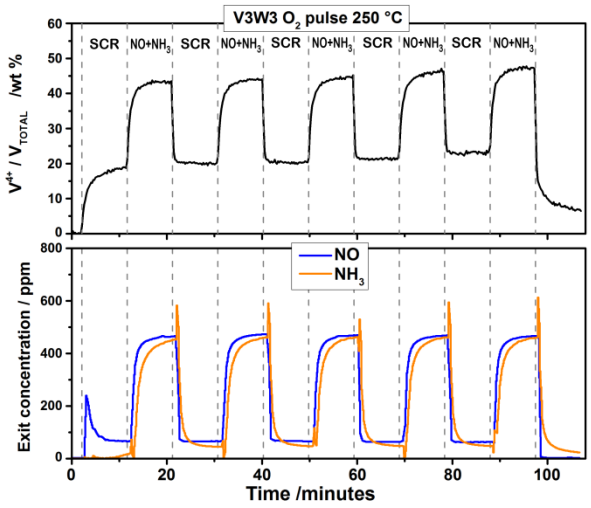

Figure 4. Top: EPR signal intensity as a function of time for the V3W3 sample during cycling between *operando* SCR and *in-situ* under NO + NH_3 (1000 ppm of each). The EPR signal intensity has been recalculated as the concentration of EPR active V(IV) relative to the total vanadium content. The starting point at t = 0 corresponds to the resting state after oxidation with O_2/He. Bottom: The composition of the exhaust gas as a function of time during the same experiment.

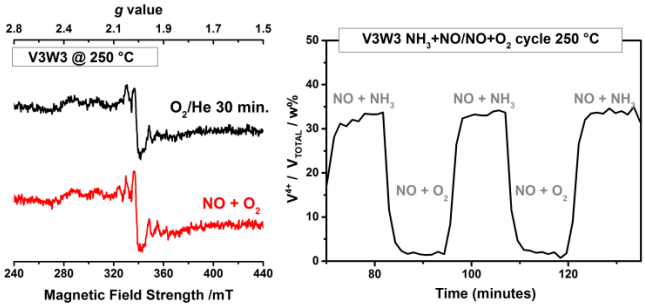

Figure 5. Left: Evaluation of the background spectra: First derivative EPR spectra of V3W3 collected at 250 °C after 20% O_2/He (black) and 1000 ppm NO + 10 % O_2 in He (red). Right: Intensity of *in-situ* EPR signal for the V3W3 sample during cycling between a flow of NO + NH_3 and a flow of NO + O_2 at 250 °C.

Spectral simulations: The experimental and simulated spectra for V3W3 under *operando* SCR at 250 °C with and without oxygen present are shown in Figure 6 (The data for all samples are collected in Table S1 and Figure S9-S10). The findings by computer simulation analysis of the spectra under *operando* SCR at 200 and 250 °C are collected in Table 2. The spectra were all reproduced using sums of three different types of species: **A**, **B** and **C**. Species **A** accounts for the majority of the EPR signal intensity: 66-99 % for all samples under all gas compositions and temperatures. **A** has a broad featureless isotropic EPR line centered at g_{iso} = 1.96. Neither the hyperfine coupling to the vanadium center nor the g anisotropy is resolved. **B** and **C**, on the other hand, have narrow lines and resolved hyperfine coupling to the ^{51}V nuclei (I = 7/2). It was assumed that the strong V=O bond induces near axial symmetry and therefore in the modeling of the spectra of **B** and **C** both g- and A-tensors are restrained to be axial with collinear main axes. For distorted surface species this

assumption may break down. It was adopted in all simulations in order to keep the model simple and any deviations are therefore assumed to be absorbed in the line width. The relative percentages of **A**, **B** and **C** were fitted under the assumption that the fitting of the line widths of each species in Easyspin was reasonable with only minor deviations. The fitted parameters of **B** and **C** deviate a little between samples and experiments. This may be due to a different distribution of subspecies of **B** and **C** that are only partially resolved or to the limitations of our fitting protocol. For the purpose of this investigation, these minor differences were ignored and they were therefore grouped as being of either **B** or **C** type.

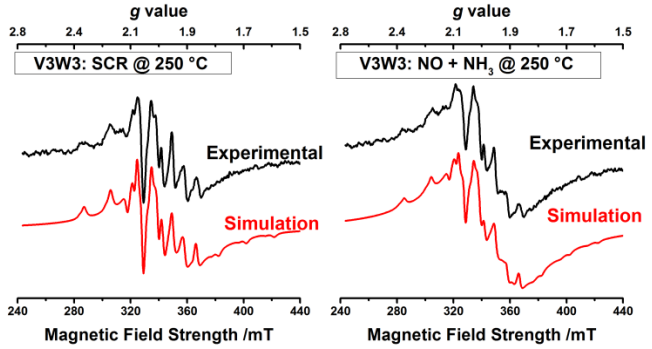

Figure 6. Experimental (black) and simulated (red) first derivative *in-situ* EPR spectra of V3W3 at 250°C. Left: *operando* SCR (NO + NH_3 + O_2); right: NO + NH_3. The intensity of the spectrum to the right is approximately twice the intensity of the spectrum on the left.

Table 2. Fitted spin Hamiltonian parameters and distributions under *operando* SCR. Column 3-8 contain fitted axial spin Hamiltonian parameters for the background corrected EPR spectra. Column 9 is the Lorentzian line width. These are identical within the uncertainty for the spectra obtained at 200 and 250 °C. Column 10-11 contain fitted distributions of EPR active species and are given relative to the total EPR spectrum intensity of that particular spectrum. The values relative to the total amount of vanadium are given in parentheses.

Samples and Species		Fitted Parameters[a]							Fitted Distributions[a]			
		$g_\perp$	$g_\parallel$	g_{iso}[b]	$A_\perp$ MHz	$A_\parallel$ MHz	A_{iso}[b] MHz	LW mT SCR 250 °C	% SCR 250 °C		SCR 200 °C	
V3W3	A	-	-	1.96	-	-	-	70	87	(20)	92	(24)
	B	1.97	1.91	1.95	190	505	295	4	10	(2)	7	(2)
	C	1.96	1.93	1.95	150	500	265	3	2	(0.5)	1	(0.3)
V6W3	A	-	-	1.96	-	-	-	85	98	(12)	97	(15)
	B	1.97	1.92	1.96	200	505	300	4	2	(0.2)	3	(0.4)
	C[c]	1.97[c]	1.96[c]	1.97[c]	155[c]	505[c]	270[c]	3[c]	0.3	(0.04)	0.7	(0.1)
V6W0	A	-	-	1.96	-	-	-	65	97	(11)	98	(15)
	B	1.97	1.92	1.95	190	500	295	4	3	(0.4)	2	(0.3)
	C[c]	1.96[c]	1.96[c]	1.96[c]	130[c]	445[c]	235[c]	3[c]	0.1	(0.01)	0.03	(0.005)
V3W0	A	-	-	1.96	-	-	-	60	66	(3)	71	(4)
	B	1.97	1.91	1.95	195	515	300	4	16	(0.7)	15	(0.8)
	C	1.96	1.93	1.95	145	465	250	4	18	(0.8)	14	(0.8)

[a]The error bars on fitted values are estimated to be 0.01 on g-values, 5-10 MHz on A-values and 1-2% on distributions. [b]g_{iso} is calculated as $g_{iso} = 1/3(2g_\perp + g_\parallel)$. A_{iso} is calculated as $A_{iso} = 1/3(2A_\perp + A_\parallel)$. [c]The content of these sites are less than 0.1 wt% of the total amount of vanadium and the spin Hamiltonian parameters are not well-determined from the fit.

X-band EPR spectroscopy is sensitive to certain types of paramagnetic centers, but a signal is not always seen even though a given species is paramagnetic. If the EPR signal can be assigned to an S = ½ species and the relaxation of the excited spin state is not too fast then it is possible to quantify the signal by comparison with a spin reference[15,35–37]. If the entire spectrum observed can be assigned to a particular species, then it is possible to quantify the amount by analysis of the EPR signal intensities. This assumption is not trivial, since other paramagnetic species can also be present. Possible signals from each metal center present on the $V_2O_5/WO_3/TiO_2$ are discussed in the following list of relevant EPR active centers:

- **Titanium(IV), vanadium(V) and tungsten(VI)** are all d^0 systems, that are diamagnetic and will always be EPR silent. After exposure to strong reductants paramagnetic titanium(III) can form. The signal from Ti(III) is expected at a line position of g = 1.93 and may require low temperatures and higher frequencies to be observed[35]. None of the spectra presented here had any features assignable to Ti(III). Tungsten(V) is also paramagnetic, but the signal is expected at even lower g-values of ~1.8 and was not observed either.
- **Vanadium(IV)** is a paramagnetic d^1 system and EPR signals are usually easily recognized by the hyperfine interaction with the I = 7/2 ^{51}V nucleus giving a characteristic pattern. The g-value and the coupling constant to the nuclear spin (the A-value), depend on the coordination sphere of vanadium, vide infra. Not all vanadium(IV) species are expected to be observable in an X-band EPR experiment at elevated temperatures. If the symmetry of the coordination sphere is tetrahedral or octahedral with similar ligands in all positions, then the ground state will be degenerate, which is not a stable situation according to the Jahn-Teller theorem. Distortions away from the high symmetry will release the degeneracy, but if the distortion is hindered by the crystal structure (i.e. by vanadium(IV) doped in the oxide of another metal) then the distortions are not able to separate the ground state and the closest excited state efficiently. As a result, vibronic coupling results in fast relaxation of the excited spin state and the EPR signal will be broadened beyond detection at elevated temperatures. For tetragonal (i.e. having a four-fold axis) oxidovanadium(IV) the $^2B_2$ ground state (C_{4v} notation) is non-degenerate and well separated from the other electronic states, so relaxation rates are slow enough for the EPR spectrum to be observed.
- **Vanadium(III)** is also paramagnetic with S = 1. EPR signals from integer spin species often have non-negligible zero-field splitting. In this case the X-band frequency is too low to see a signal. Vanadium(III) EPR signals on V_2O_5/TiO_2 have only been observed at cryogenic temperatures with high frequency high field EPR.[35]
- **Dimeric oxidovanadium(IV)** species are expected to couple antiferromagnetically resulting in an S = 0 ground state and an S = 1 excited state. If the coupling is strong enough only the ground state is populated, and the dimer will be EPR silent. For oxidovanadium(IV) species connected with a μ-oxido bridge the coupling is expected to be strong enough to result in loss of the EPR spectrum. For longer diamagnetic bridges,

such as -O-V(V)-O- or similar, the interaction is very weak and the EPR spectrum will correspond closely to the spectrum of an oxidovanadium(IV) monomer, but the interaction with the neighboring paramagnetic centers results in increased line width.

We argue that, in this work, tetragonal oxidovanadium(IV) are the only species giving a significant EPR signal since:

- The observed spectra correspond well to tetragonal oxidovanadium(IV) species and this can account for all of the observed EPR spectral intensity.[38]
- All spectra were obtained at room temperature or above, where many of the other possible EPR signals would be unobservable.
- The EPR response follows the gas flow. Under oxidizing conditions no signal is observed. Under reducing SCR conditions, a large EPR response is seen.

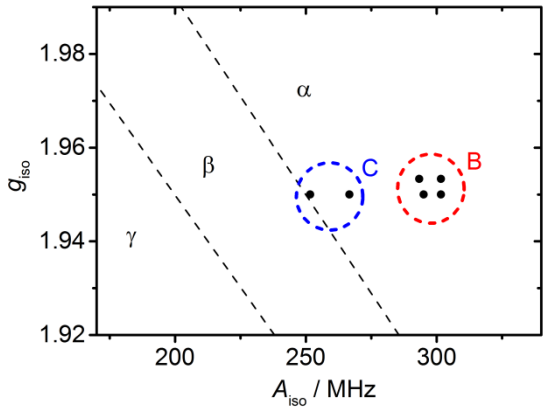

Figure 7. Correlation diagram – g_{iso} vs. A_{iso} for vanadium(IV) species. The individual components of the four samples in Table 2 with well-determined spin Hamiltonian parameters are plotted. The diagram is based on Davidson and Che.[39]

Identity of observed VO^{2+} species: The spin Hamiltonian parameters are indicative of the coordination environment of the vanadium(IV) species. As an analogue to the Blumberg-Peisach plot[40], which has been successful in grouping the EPR signals of copper species according to the coordination environment, Goodman and Raynor[41] and Davidson and Che[39] suggested to plot the g-values of V_2O_5/TiO_2 species averaged over the three molecular axes, g_{iso} as a function of the corresponding averaged hyperfine coupling constants, A_{iso}. Analyzing data from literature, the different EPR active vanadium(IV) species were plotted and shown to separate into three areas in the plot each area being indicative of different coordination environments of the vanadium centers. The α area is characteristic of oxidovanadium(IV): VO^{2+} with tetragonal symmetry, the oxido group being in the apical position and 4 donors in the plane perpendicular to the V=O bond. A sixth ligand may also be present *trans* to the oxido group. In the present case the 4 or 5 additional ligands could be water, hydroxide, oxygens from the support, bridging oxido or hydroxido groups to other V or W centers. The β area is characteristic of vanadium ions in near tetrahedral geometry and the γ area is characteristic of vanadium ions in near octahedral symmetry. The species giving sharp and well defined EPR signals in this work are all found within the α area, see Figure 7. The results fall in two groups: **B** and **C** as indicated in Figure 7. Species **B** has the spin Hamiltonian parameters $g_{\perp}$ = 1.97, $g_{||}$ = 1.915±0.005, $A_{\perp}$ = 195±5 MHz and $A_{||}$ = 510±5 MHz. It accounts for 10 and 16 % of the total EPR active V(IV) at *operando* SCR at 250 °C in the two samples with low loading of V, but is below 3 % for the samples with high content of V. Species **C** has the parameters $g_{\perp}$ = 1.965±0.005, $g_{||}$ = 1.945±0.015, $A_{\perp}$ = 150±5 MHz and $A_{||}$ = 483±23 MHz and is only present in significant amounts in the V3W0 sample where is accounts for 18 % of the EPR active vanadium. The spin Hamiltonian parameters of the different species and the distribution of species is essentially the same as observed by Vuong et. al. by operando EPR on a similar material.[16]

Species **A** is assigned to magnetically interacting or otherwise broadened oxidovanadium(IV) centers due to the unresolved EPR signal of this species. Species **B** and **C** are assigned to *magnetically* isolated tetragonal oxidovanadium(IV) species that may or may not be isolated in a *structural* sense as well. Magnetically isolated means that all the closest metal centers are diamagnetic: Ti(IV), V(V), W(VI). Structurally isolated denotes that the V(IV) center are not connected through an oxido bridge to any other vanadium centers.[42]

Species **B** and **C** have been discussed and assigned on the basis of the EPR spectrum in the literature by several authors and we will continue the discussion in the following: The spectrum of species **B** is very similar to several literature-reported spectra that are assigned by Paganini et al.[10] to be 5-coordinate surface oxidovanadium(IV) species with an (equatorial) empty coordination position that has the possibility to interact with adsorbates. Arnason et al.[22] suggest that species **B** is a 5-coordinate partially hydrolyzed oxidovanadium(IV) surface species on the surface of the anatase with a weak sixth interaction trans to the oxido group.

Species **C** was assigned by Paganini et al.[10] to be five- or six-coordinated oxidovanadium(IV) with a stronger interaction or insertion into the TiO_2 matrix. The parameters of species **C** are also very similar to the values found for a species assigned as 5- or 6 coordinated V(IV) in intralattice positions in TiO_2.[39] Arnarson et. al.[22] suggested that species **C** correspond to a pseudo-tetrahedral 4-coordinate oxidovanadium(IV) species present on other facets of the anatase crystallite. It can be discussed if such a species would be EPR active at high temperatures since fast spin-lattice relaxation may broaden the EPR signal beyond detection for species with electronically excited states that are too close to the ground state. This would be the case for a trigonal 4-coordinate oxidovanadium(IV) species.

In order to pursue the assignment of these species a little further the assignment in molecular vanadium coordination chemistry has been consulted.[44] The spin Hamiltonian parameter $A_{||}$ for oxidovanadium(IV) species has been found to follow an additivity relationship, which also holds up well under slight distortions of the coordination sphere away from tetragonal. The value of $A_{||}$ is empirically found to be a sum of a contribution for each of the 4 close non-oxido donors for oxidovanadium(IV) species.[45] Hydroxido and alkoxido, RO^- groups are both tabulated to have a

contribution of $39 \cdot 10^{-4}$ cm^{-1} whereas water has a contribution of $46 \cdot 10^{-4}$ cm^{-1}. The $A_{||}$ value of species **C** (483 MHz or $161 \cdot 10^{-4}$ cm^{-1}) correspond to 4 donors with an average value of $40 \cdot 10^{-4}$ cm^{-1}, whereas the one of species **B** (510 MHz or $170 \cdot 10^{-4}$ cm^{-1}) corresponds to an average of $43 \cdot 10^{-4}$ cm^{-1}. This corresponds well to the assignment of Arnarson et. al. for species **B** and to the assignment of Paganini et. al. for species **C**. In accordance with this we suggest that the difference between species **B** and **C** is not the coordination number but rather the degree of hydrolysis; **B** being more hydrolyzed than **C** by having more hydroxido groups or having hydroxido bridges to neighboring metal centers rather than oxido bridges. Highly hydrolyzed species are only found on the surface, whereas the less hydrolyzed species can either have a strong interaction or insertion into the support or it could be an efficiently dehydrated surface species.

It is not possible to place species **A** in the plot in Figure 7 since the hyperfine coupling is not resolved. The g-value is very similar to the average of the g-values in both species **B** and **C** and is similar to the one found for V(IV) defects in amorphous V_2O_5, which also has a tetragonal structure around V.[46] Species **A** is expected to have the same type of coordination environment as species **B** and **C**, but experience severe broadening of the EPR spectrum due to interaction with other paramagnetic centers. Neither the individual hyperfine lines nor the differences that allowed the differentiation between type **B** and **C** sites are resolved. There are several possible reasons for the broadening: Magnetic exchange with nearby V(IV) species at high V(IV) concentrations result in severe broadening of EPR spectra but other effects might also be relevant given the high temperatures in the *in-situ* investigation: Vanadium in non-crystalline surface species may have a high level of distortions in the coordination environment. Species with vibrationally active –OH or H_2O groups are also expected to be broadened. In this work, the line width was observed to increase significantly with increasing concentration of oxidovanadium(IV) as the sample was reduced, see Figure 3, and therefore we assess the magnetic exchange to be the most important factor for the observed broadening.

If vanadium would be found as tetrahedral or octahedral non-oxido V(IV), these would be expected to be subject to the same effect as described above for trigonal oxidovanadium(IV) species. The effect of close-lying excited states can cause the EPR signal of V(IV) to disappear completely at elevated temperatures due to fast relaxation. If some V(IV) has diffused completely into an ideal TiO_2 lattice position, as reported to be relevant after annealing at high temperatures, the EPR signal would belong to the γ area in Figure 7, but would likely be unobservable at our experimental conditions. Likewise, for tetrahedral non-oxido V(IV) with parameters in the β area of Figure 7. EPR used as described here is expected only to be sensitive to tetragonal oxidovanadium(IV) species, and it should be noted that a positive identification of these species is shown here, and they have a quite high abundance.

EPR active V(IV) observed during operando and in-situ SCR conditions: The relative intensity of EPR signals throughout an experiment can be obtained from the double integral when care is taken to assure accurate measurements. The relative intensities throughout single experiments were identical within the given uncertainty across several replicates. The relation to the total amount of vanadium in the sample is more challenging and connected with a higher uncertainty, but it is necessary for the discussion regarding the relevance of tetragonal oxidovanadium(IV) for the SCR reaction. It is imperative to asses if the vanadium EPR signal observed corresponds to a significant fraction or only traces of the vanadium in the sample. Our procedure is detailed in the experimental section. The amount of EPR active vanadium during different experimental conditions at 250 and 200 °C are given in Figure 8. The precise value of the V(IV) amount has some uncertainty, the existence and the relative high levels of V(IV) are non-debatable due to the strong and recognizable EPR response.

The first thing to note is that the amount of vanadium, which can be reduced *in-situ* under a flow of NO + NH_3 at 200 or 250 °C is quite substantial for V3W3 with approximately 43 % of the total vanadium in the sample at both 200 or 250 °C. For the 3 other samples the amount is around 20 %. This amount is termed the *redox accessible vanadium*. For the application of the catalyst another relevant measure is the amount of *redox accessible* vanadium per *weight of catalyst material* including support material. This parameter could be the target for optimization in an industrial context. Recalculating the numbers from Figure 8 will achieve the following amounts of redox accessible vanadium: 0.78 w% for V3W3, 0.72 w% for V6W3, 0.63 w% for V6W0 and only 0.34 w% for V3W0. Clearly V3W3 is the most reducible material. This determination using EPR represents a quantitative lower bound for the reducibility of the catalyst and the results could be compared with e.g. H_2-TPR results for the same material.[47] The reducibility by EPR has been tested with an SCR-relevant gas mixture, whereas the reducibility tested with hydrogen gas is a model experiment, which is far away from actual SCR conditions.

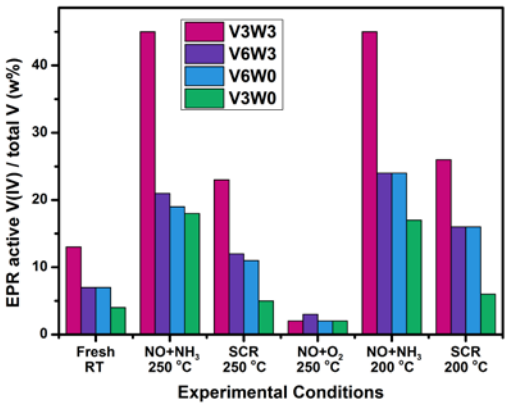

Figure 8. The amount of EPR active V(IV) measured at steady state conditions during the experiments for all samples. The numbers are given as weight percentages of the total vanadium content.

In order to investigate the development in the amount of EPR active oxidovanadium(IV) as a function of temperature the samples were exposed to *operando* SCR (NO + NH_3 + O_2) at several temperatures. The results are given in Figure 9.The

amount of oxidovanadium(IV) under *operando* SCR relative to the total catalyst weight is significantly lower for V3W0 compared to the other samples. The presence of either the tungsten promoter or a high vanadium concentration is seen to enhance the reducibility of the vanadium on the catalyst, thus resulting in the observed higher V(IV) content.

The amount of EPR active oxidovanadium(IV) found under *operando* SCR is obtained on an active catalyst, where the concentration of NO and NH_3 in the gas phase is not the same in the beginning and in the end of the catalyst bed. The EPR signal is accumulated over the entire sample and the amount of oxidovanadium(IV) found is therefore dependent on the ratio between the rate of the reduction and oxidation reactions, which have different activation energies and temperature dependences. The EPR signal is also dependent on the conversion over the bed if the assumption of a differential reactor condition does not hold at temperatures when the conversion is high.

The distribution between the reduced and oxidized resting states of the catalyst changes with temperature and experimental conditions. This is a consequence of several factors e.g. reduction rate, oxidation rate, space velocity, ammonia adsorption, water content etc. A maximum in the oxidovanadium(IV) concentration is observed in Figure 9 at around 200 °C for all four samples. This observation has high confidence. We have not tried to interpret this behavior at this stage, however, since it would require further data and investigations at a wider range of experimental conditions.

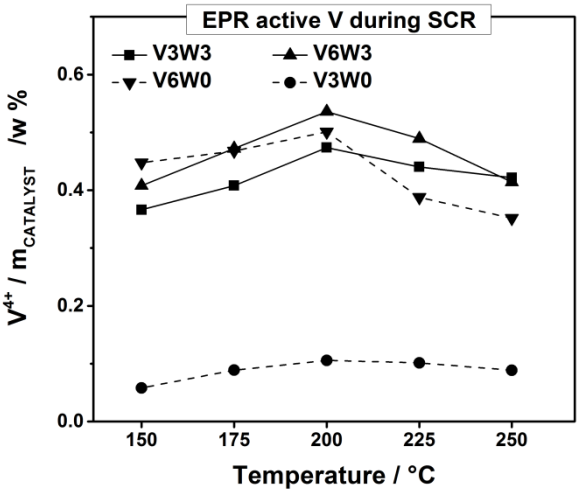

Figure 9. The EPR active vanadium content during *operando* SCR at different temperatures given in weight percentage of the total catalyst mass including support material.

Distribution of vanadium species during in-situ and operando SCR conditions: The distribution between magnetic non-interacting monomers, **B** and **C** and the magnetically interacting species giving an isotropic EPR spectrum, **A** is difficult to determine since the distribution found will depend on the linewidth used in the simulation of the spectra. The first-derivative spectra normally given for EPR spectra, see Figure 6, cause the contributions from sharp lines to appear more dominant than they are in reality. The analysis using computational simulations is necessary in order to assess the distribution. In the data reported here the line width was fitted along with the spin Hamiltonian parameters. The data are given in Figure 10 for all samples under *operando* SCR and *in-situ* under NO + NH_3 flow at 250 °C. In these materials the species giving a broad featureless signal is always the majority, and this does not change during SCR at different temperatures (see Table S2 and Figure S11). The ratio of the amount of **B** + **C** to the amount of **A** is higher for the V3 than for the V6 samples, both in the reduced state and under *operando* SCR, see Figure 10. Since the degree of uncertainty is quite high for the simulation of these species, this could be a result of the resolution or error in simulations, but it could also indicate a higher degree of clustering of paramagnetic species for the high loading samples.

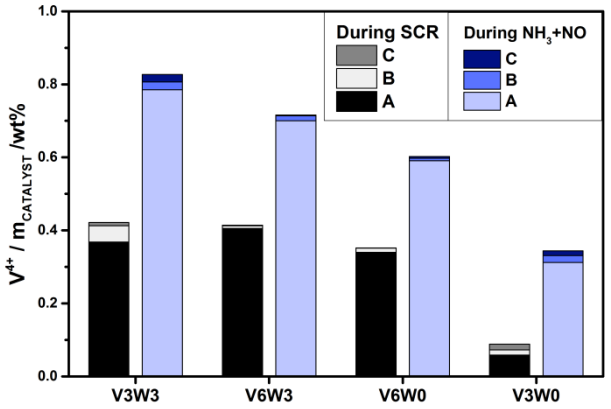

Figure 10. Content of EPR active oxidovanadium(IV) and distribution of the different oxidovanadium(IV) species relative to the total weight of the catalyst under *operando* SCR (grey columns) and under *in-situ* NO + NH_3 (blue columns) at 250 °C.

Tetrahedral V compounds have been found by Lewandowska et al.[9] and Eckert and Wachs[48] using ^{51}V-NMR spectroscopy. NMR investigations are only sensitive to diamagnetic V(V) species that are generally accepted to be more in favor of tetrahedral coordination than V(IV). Nevertheless, it is reasonable to suggest that both 4-, 5-, and 6-coordinate species of V in both oxidation states can be coexisting with the distribution depending on the V content, W content, temperature, extent of hydration, gas composition etc. In V_2O_5 type phases in bulk or on the surface of support materials the oxido group is normally ubiquitous. This should hinder the formation of highly symmetric tetrahedral or octahedral non-oxido species. The presence of these sites cannot be excluded based on EPR investigations alone since they would not be observed. This must be considered when making conclusions regarding the V phases present. If some vanadium has entered the framework of the anatase support to obtain a higher symmetry site by substituting for titanium, it is likely not relevant for the SCR reaction cycle. The inability of EPR to observe these sites will not change the conclusions or quantifications of the sites that are accessible for the SCR reaction. The percentages of V present as oxidovanadium(IV) collected in Figure 8 are quite substantial compared to the total

vanadium content but there might still be additional EPR silent V(IV) phases present that cannot be observed. The amount of these sites in fresh and used samples could be assessed by comparing EPR spectra obtained at elevated temperature with spectra obtained at cryogenic temperatures where the lifetime of the exited state may be sufficient long to observe these phases. At this stage the experiment has not been performed.

Alternating between NO + O_2 and NO + NH_3 flows at 250 °C for all four samples show that NO + NH_3 reduce a substantial percentage of the total amount of vanadium present to give the EPR active oxidovanadium(IV), see Figure 5 right, for the results for V3W3 (Figure S4 for the rest). A reoxidation occurs in NO + O_2, where essentially all vanadium is oxidized to EPR inactive vanadate(V). Both the reduction and the oxidation are too fast to follow at 250 °C with this experimental protocol. From these experiments it is not possible to make any conclusions regarding the relative rates of oxidation and reduction, or to observe any intermediate species.

The oxidation with O_2 alone is not distinguishable from an oxidation with NO + O_2 except for a trace of V(IV) remaining on the sample when oxidizing with O_2 alone (see Figure S7). If a catalyst is first exposed to O_2 at 250 degrees for a period and then is exposed to NH_3 alone at 200 °C, the generation of EPR active oxidovanadium(IV) is not observed (see Figure S12). It cannot be precluded from these data that reduction of vanadium is taking place with ammonia alone, but it is suggested that it is not resulting in the same EPR active oxidovanadium(IV) species that were the result when the catalyst was exposed to NO and NH_3 together.

During the oxidation in NO + O_2 a nitrate-nitrite equilibrium in the cycle has been suggested[27] and experimentally observed by IR spectroscopy on vanadia SCR catalysts[49]. According to the SCR cycle suggestion[24], a nitrate species on the redox site is predicted only when vanadium is in the EPR silent V(V) state. This hypothesis was challenged by first exposing the sample to NO + O_2 and then to NO alone during an *in-situ* EPR experiment. Only a negligible change was observed in the EPR spectrum of the vanadium-based SCR catalyst during this procedure (see Figure S8). The absence of any EPR active nitrate species is in accordance with the hypothesis.

Conclusions

$V_2O_5/WO_3/TiO_2$ catalysts have been investigated under conditions relevant for the SCR reaction in a fixed bed plug flow reactor operating at 420,000 h^{-1} running with a NO conversion of up to 85 % at 250 °C. The findings reported here show that up to 45 % of the total vanadium present in the catalyst can be reduced to tetragonal 5- or 6-coordinate oxidovanadium(IV) species by NO and NH_3 together. During *operando* SCR up to 26 % oxidovanadium(IV) are observed. With this we provide unambiguous evidence of the presence of V(IV) species during *operando* SCR and underline their importance for the SCR catalysis. Furthermore, the results provide evidence that a large percentage of reduced vanadium is indeed present as oxidovanadium(IV), VO^{2+} species. The high ratio of oxidovanadium(IV) present after reduction also implies that the hypothesis that reduction of oxidovanadium(V), VO^{3+} leads to non-oxido V(IV)-OH - as often proposed in the literature[1] is incorrect. It is proposed in accordance with Wachs et al.,[3] that the double bond of the oxidovanadium unit is not broken during catalytic turn-over in the SCR reaction. This is also in line with the argument that the V=O double bond is the most stable bond within the vanadia structure.

The importance of using sufficiently high space velocities during *operando* SCR studies has been clearly demonstrated in this work. If the catalyst is running too close to complete conversion the difference in rate between the reduction and oxidation step is equalized by mass transfer limitations and the reaction could be running in only the upstream part of the catalyst bed whereas the downstream part is in the oxidized state.[50]

The amount of oxidovanadium(IV) species that give sharp, well-defined signals in the EPR spectrum is relatively small. The majority of the observable oxidovanadium(IV) species have a severely broadened EPR spectrum, probably due to magnetic exchange interactions with neighboring paramagnetic sites. These sites could be other vanadium(IV) species, but it should be remembered that NO and O_2 are also paramagnetic and may influence the line width of surface species. Other reasons for broad lines are also suggested but are likely less important: High levels of structural distortions of the oxidovanadium(IV) sites and vibrationally active OH^- or H_2O groups coordinated to VO^{2+}. The local coordination environment of the vanadium sites giving sharp lines (**B** and **C**) and the ones giving broad lines (**A)** are not suggested to be much different; all are suggested to be roughly tetragonal with the oxido group in the apical position – only the magnetic coupling pattern is different leading to broader EPR lines for the **A** sites.

Using the additivity principle[44] for the magnitude of the hyperfine coupling in tetragonal oxidovanadium(IV) compounds, **B** is suggested to be magnetically and structurally isolated 5- or 6-coordinate surface oxidovanadium(IV) species and **C** is suggested to be magnetically isolated oxidovanadium(IV) species in less hydrolyzed but still 5- or 6-coordinate sites. The assignment of EPR signals to particular sites are still under discussion.[10,22] When structurally polymeric surface layers are formed at higher vanadia or combined vanadia/tungsta loadings the amount of species **C** becomes insignificant.

The content of reduced vanadium species under *operando* SCR is high for samples with high V content and/or containing WO_3, and lower for the V3W0 sample. Thus, we conclude that the WO_3 promoter enhances the overall reducibility of the catalyst, so that a good reducibility - and thereby activity of the catalyst - can be obtained even at low V content.

Experimental Section

Catalyst materials: Fiberglass plates wash coated with TiO_2 (anatase) were calcined at 500 °C and then impregnated with oxidovanadium(IV)oxalate, $VO(C_2O_4)\cdot xH_2O$ and ammonium metatungstate, $(NH_4)H_2W_{12}O_{40}\cdot xH_2O$ (both from Sigma-Aldrich). After drying they were again calcined in air at 400 °C. The plates were broken up, separated roughly from the fibers and fractioned to particle sizes

between 150 and 300 µm. The sieve fraction and flow rate was chosen relative to the reactor dimension such that a plug flow was obtained. The materials are highly active in the SCR reaction and are made in the same way as reported in a number of publications since [7].

4 samples were tested; V3W3, V3W0, V6W3 and V6W0, where the numbers refer to the approximate content of V_2O_5 and WO_3 in the sample in wt %. The exact content of V and W in the final fractioned material was determined by inductively coupled plasma atomic emission spectroscopy (ICP-OES) using a Perkin Elmer Optima 7300 DV.

Raman spectra were obtained on sieved fractions (150–300 µm) of pelletized (around 0.5 tons/cm) samples placed in a Linkam CCR1000 *in-situ* reactor in air flow and at 250 °C. The spectra were recorded on a Horiba-Jobin Yvon LabRam HR equipped with a 488 nm (visible blue line) laser. A confocal microscope (10x) was used to focus the laser on the sample. The Raman spectra show no sign of the presence of crystalline V_2O_5 or WO_3 phases in any samples, confirming an efficient dispersion of both vanadium and tungsten on the anatase support. FTIR spectra were recorded on a Bio-Rad FTS575C. 100 g of sample was sieved and pressed to create a self-supporting wafer which was heated to 400 °C in 15% O_2/Ar air flow for 14 h and then cooled and evacuated before recording the spectra. BET surface area was measured by N_2 adsorption in a Micromeritics ASAP2000.

In-situ EPR: The *in-situ* EPR set-up consists of two independent flow systems with Brooks mass flow controllers connected to a four-way valve controlling the flow to a quartz reactor positioned in the cavity of a Bruker X-band EMX EPR spectrometer equipped with a ST4102 cavity. The frequency was close to 9.4 GHz, modulation amplitude 100 kHz, microwave power 6.5 mW and time constant 10.24 ms, the field was varied between 240 and 460 mT. The EPR spectrometer was connected to a Bruker variable temperature unit capable of heating the sample tube to 250°C using a flow of air. The exhaust gas was connected to a Thermo 17C NH_3 converter and analyzer for *operando* measurements. A simplified sketch is seen in Figure 11.

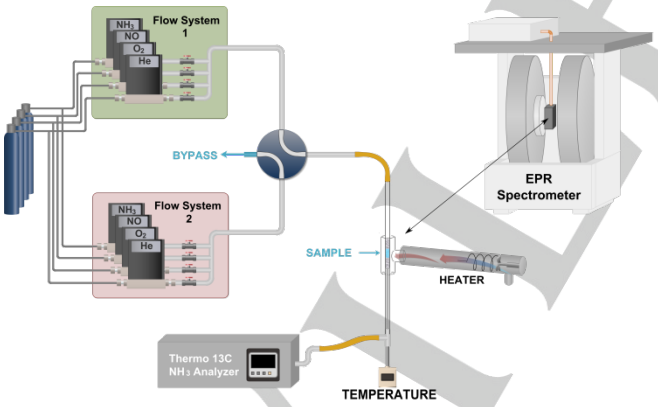

Figure 11: Simplified illustration of the *operando* EPR setup

A known amount of sample (15 – 30 mg) was immobilized between two quartz wool plugs in a simple quartz tube reactor with outer diameter of 5 mm and inner diameter of 3 mm. The total gas flow through the sample was kept at 200 NmL/min for all experiments. The packed sample was tested for pressure drop. The EPR signal of the as-prepared sample was recorded at room temperature and simulated to obtain the $I(T_{start})$ intensity needed for the quantitative determination throughout the experiment. The spectra and their simulations are found in Figure S13. The sample was then heated to 250 °C under an O_2/He flow (20 % O_2) and was kept there for at least 30 minutes to ensure complete oxidation. The EPR spectrum of the fully oxidized sample (collected as an average of 10 individual spectra) was subtracted from all following spectra. The small remnant spectrum of unreactive V(IV) and impurity signals from the support were negligible in good correspondence with a complete oxidation of the catalyst. This procedure was found to improve the baseline, which is important for quantitative determination of EPR signal. The subtracted spectra are shown in Figure S6. Several series of experiments were performed on the oxygen activated samples. The EPR spectra were measured continuously during the duration of the measurement with a resolution of 1024 points and a measurement time of about 15 seconds per field sweep. The intensity of the EPR spectra for all experiments was obtained by double integration of the measured first-derivative background-corrected EPR signal over the measured field range (See SI for further details on data and calculations). All double integrated spectra were examined to assure their shape followed a sigmoid curve and background corrections were applied when necessary. The amount of V(IV) relative to the total amount of vanadium V_{total} (Table 1) was calculated throughout the experiments using the equation below. The EPR signal intensity of the fresh catalyst material, I_{start} and the amount of EPR active V(IV) in the fresh catalyst, V(IV)(fresh) determined during the quantification, goes into the equation along with the temperature throughout the experiment, T.[13]

$$\frac{\mathrm{V(IV)}}{\mathrm{V}_{total}} = \frac{I(T)}{I_{start}} \cdot \frac{T}{T_{start}} \cdot \frac{\mathrm{V(IV)}(fresh)}{\mathrm{V}_{total}}$$

All four samples have been treated exactly the same way and conclusions based upon comparisons between the developments in the intensity of the EPR spectra of the samples have high confidence.

NO+NH₃/operando SCR cycle experiments: One flow contained a standard SCR feed of 5 % O_2, 500 ppm NO, 500 ppm NH_3 and balance He. The other flow contained NO + NH_3 in the same concentrations but did not contain O_2. The gasses did not contain added water. The gas flows were switched close to the sample by turning the 4-way valve approximately every 10 minutes for about 2 hours at 250 °C. Subsequently, the flow was switched to pure O_2 while the temperature was changed to a lower value. The full switching experiments were also performed at 200 °C; *operando* SCR was maintained for 20 minutes at 225 °C between the two full experiments and at 175 and 150 °C after the last full experiment. The exit gas composition was measured by a Thermo 17C NH_3 analyzer during the full experiment, which took around 9 h in total.

NO+NH₃/NO+O₂ cycle experiments: One flow contained NO + NH_3 each at 1000 ppm and balance He, the other contained NO + O_2 at 1000 ppm and 5 %, respectively and balance He. The flow was switched every 10 minutes for a few cycles at 250 °C.

Quantification experiments: A series of standard samples of $VOSO_4 \cdot 3H_2O$ (Sigma-Aldrich) in a solid solution of K_2SO_4 were measured at room temperature (RT) in standard 4 mm suprasil quartz EPR tubes. Identical amounts of all 4 catalyst samples in Table 1 were measured under completely identical settings and tube positions. The experiment was performed three times, giving the amount of EPR active V(IV) in the fresh catalyst, V(IV)(fresh). The results are given in Figure S14-S15 and Table S3, where a more detailed description of the quantification procedure also can be found.

For the *operando* experiments, the entire catalyst bed was monitored with EPR while exposed to different gas mixtures. The catalyst was mounted in a plug flow reactor with a well-defined particle size. The reactor and flow were dimensioned in order to keep the conversion of NO well below 85 % when running *operando* SCR and these conditions were then kept constant for all experiments. Care was taken to not run too close to full conversion since otherwise part of the catalyst bed could be in an inactive resting state which could dominate the measured spectra. The term

operando will only be used when the measurement of the exhaust gas shows that NO and NH_3 are being consumed.

EPR spectra were simulated using the software package Easyspin.[51] The parameters fitted for each species are axial g-values: $g_{\perp}$, $g_{||}$, hyperfine coupling constants $A_{\perp}$, $A_{||}$ and line width parameters in the standard axial spin Hamiltonian (S = 1/2) under the assumption of Lorentzian line shapes.

Acknowledgements

This work was financially supported by the Danish Independent Research Council DFF − 1335-00175 and the Innovation Fund Denmark (IFD) - 6151-00008B (Pro-NOx). Carlsbergfondet is acknowledged for supporting the upgrade of the EPR instrument at Department of Chemistry, DTU.

Keywords: Catalysis • EPR Spectroscopy • *Operando* Spectroscopy • SCR • Vanadium

[1] M. Inomata, A. Miyamoto, Y. Murakami, *J. Catal.* **1980**, *62*, 140–148.

[2] G. Ramis, G. Busca, F. Bregani, P. Forzatti, *Appl. Catal.* **1990**, *64*, 259–278.

[3] I. E. Wachs, G. Deo, B. M. Weckhuysen, A. Andreini, M. A. Vuurman, M. de Boer, M. D. Amiridis, *J. Catal.* **1996**, *161*, 211–221.

[4] G. Ramis, L. Yi, G. Busca, *Catal. Today* **1996**, *28*, 373–380.

[5] U. S. Ozkan, Y. Cai, M. W. Kumthekar, *J. Phys. Chem.* **1995**, *99*, 2363–2371.

[6] N.-Y. Topsoe, *Science.* **1994**, *265*, 1217–1219.

[7] N. Y. Topsoe, H. Topsoe, J. A. Dumesic, *J. Catal.* **1995**, *151*, 226–240.

[8] N.-Y. Topsøe, J. A. Dumesic, H. Topsøe, *J. Catal.* **1995**, *151*, 241–252.

[9] A. E. Lewandowska, M. Calatayud, F. Tielens, M. A. Bañares, *J. Phys. Chem. C* **2013**, *117*, 25535–25544.

[10] M. C. Paganini, L. Dall'Acqua, E. Giamello, L. Lietti, P. Forzatti, G. Busca, *J. Catal.* **1997**, *166*, 195–205.

[11] J. Soria, a. Martinez-Arias, a. Martinez-Chaparro, J. C. Conesa, Z. Schay, *J. Catal.* **2000**, *190*, 352–363.

[12] V. Lagostina, M. C. Paganini, M. Chiesa, E. Giamello, *J. Phys. Chem. C* **2019**, *123*, 7861–7869.

[13] A. Brückner, *Chem. Soc. Rev.* **2010**, *39*, 4673–4684.

[14] M. Santhosh Kumar, M. Schwidder, W. Grünert, U. Bentrup, A. Brückner, *J. Catal.* **2006**, *239*, 173–186.

[15] M. Wark, A. Brückner, T. Liese, W. Grünert, *J. Catal.* **1998**, *175*, 48–61.

[16] T. H. Vuong, J. Radnik, J. Rabeah, U. Bentrup, M. Schneider, H. Atia, U. Armbruster, W. Grünert, A. Brückner, *ACS Catal.* **2017**, *7*, 1693–1705.

[17] A. E. Lewandowska, M. Calatayud, F. Tielens, M. A. Bañares, *J. Phys. Chem. C* **2011**, *115*, 24133–24142.

[18] J. Due-Hansen, S. B. Rasmussen, E. Mikolajska, M. A. Bañares, P. Ávila, R. Fehrmann, *Appl. Catal. B Environ.* **2011**, *107*, 340–346.

[19] M. Zhu, J.-K. Lai, U. Tumuluri, M. E. Ford, Z. Wu, I. E. Wachs, *ACS Catal.* **2017**, 8358–8361.

[20] M. Zhu, J.-K. Lai, U. Tumuluri, Z. Wu, I. E. Wachs, *J. Am. Chem. Soc.* **2017**, *139*, 15624–15627.

[21] A. L. Godiksen, S. B. Rasmussen, *Catal. Today* **2019**, *336*, 45–49.

[22] L. Arnarson, S. B. Rasmussen, H. Falsig, J. V. Lauritsen, P. G. Moses, *J. Phys. Chem. C* **2015**, *119*, 23445–23452.

[23] D. C. Crans, J. J. Smee, E. Gaidamauskas, L. Yang, *Chem. Rev.* **2004**, *104*, 849–902.

[24] G. Busca, L. Lietti, G. Ramis, F. Berti, *Appl. Catal. B Environ.* **1998**, *18*, 1–36.

[25] V. I. Pârvulescu, P. Grange, B. Delmon, *Catal. Today* **1998**, *46*, 233–316.

[26] A. Marberger, D. Ferri, M. Elsener, O. Kröcher, *Angew. Chemie - Int. Ed.* **2016**, *55*, 11989–11994.

[27] L. Arnarson, H. Falsig, S. B. Rasmussen, J. V. Lauritsen, P. G. Moses, *J. Catal.* **2017**, *346*, 188–197.

[28] U. Balachandran, N. G. Eror, *J. Solid State Chem.* **1982**, *42*, 276–282.

[29] M. A. Bañares, M. Martínez-Huerta, X. Gao, I. E. Wachs, J. L. G. Fierro, *Stud. Surf. Sci. Catal.* **2000**, *130 D*, 3125–3130.

[30] G. Busca, *J. Raman Spectrosc.* **2002**, *33*, 348–358.

[31] I. E. Wachs, B. M. Weckhuysen, *Appl. Catal. A Gen.* **1997**, *157*, 67–90.

[32] M. A. Vuurman, I. E. Wachs, A. M. Hirt, *J. Phys. Chem.* **1991**, *95*, 9928–9937.

[33] T. V. W. Janssens, H. Falsig, L. F. Lundegaard, P. N. R. Vennestrøm, S. B. Rasmussen, P. G. Moses, F. Giordanino, E. Borfecchia, K. A. Lomachenko, C. Lamberti, S. Bordiga, A. Godiksen, S. Mossin, P. Beato, *ACS Catal.* **2015**, *5*, 2832–2845.

[34] A. Godiksen, P. N. R. Vennestrøm, S. B. Rasmussen, S. Mossin, *Top. Catal.* **2017**, *60*, 13–29.

[35] A. Dinse, C. Carrero, A. Ozarowski, R. Schomäcker, R. Schlögl, K.-P. Dinse, *ChemCatChem* **2012**, *4*, 641–652.

[36] R. Aasa, *J. Chem. Phys.* **1970**, *52*, 1612.

[37] T. Chang, *Magn. Reson. Rev.* **1984**, *9*, 65–124.

[38] C. V Grant, W. Cope, J. A. Ball, G. G. Maresch, B. J. Gaffney, W. Fink, R. D. Britt, *J. Phys. Chem. B* **1999**, *103*, 10627–31.

[39] A. Davidson, M. Che, *J. Phys. Chem.* **1992**, *96*, 9909–9915.

[40] J. Peisach, W. E. Blumberg, *Arch. Biochem. Biophys.* **1974**, *165*, 691–708.

[41] B. A. Goodman, J. B. Raynor, *Adv. Inorg. Chem. Radiochem.* **1970**, *13*, 135–362.

[42] V. Luca, D. J. MacLachlan, R. Bramley, *Phys. Chem. Chem. Phys.* **1999**, *1*, 2597–2606.

[43] S. Koust, L. Arnarson, P. G. Moses, Z. Li, I. Beinik, J. V. Lauritsen, S. Wendt, E. Palomares, V. Matolin, D. Fujita, R. Perez, O. Custance, A. H. Larsen, L. Lehtovaara, M. Ljungberg, O. Lopez-Acevedo, P. G. Moses, J. Ojanen, T. Olsen, V. Petzold, N. A. Romero, J. Stausholm-Moller, M. Strange, G. A. Tritsaris, M. Vanin, M. Walter, B. Hammer, H. Hakkinen, G. K. H. Madsen, R. M. Nieminen, J. Norskov, M. Puska, T. T. Rantala, J. Schiotz, K. S. Thygesen, K. W. Jacobsen, *Phys. Chem. Chem. Phys.* **2017**, *19*, 9424–9431.

[44] K. Wüthrich, *Helv. Chim. Acta* **1965**, *48*, 779–790.

[45] T. S. Smith, R. LoBrutto, V. L. Pecoraro, *Coord. Chem. Rev.* **2002**,

228, 1–18.

[46] M. Nabavi, C. Sanchez, J. Livage, *Philos. Mag. Part B* **1991**, *64*, 941–953.

[47] A. Bukowski, L. Schill, D. Nielsen, S. Mossin, A. Riisager, J. Albert, *React. Chem. Eng.* **2020**, *5*, 935–948.

[48] H. Eckert, I. E. Wachs, *J. Phys. Chem.* **1989**, *93*, 6796–6805.

[49] C. Ciardelli, I. Nova, E. Tronconi, D. Chatterjee, B. Bandl-Konrad, *Chem. Commun.* **2004**, 2718–2719.

[50] T. Günter, D. E. Doronkin, A. Boubnov, H. W. P. Carvalho, M. Casapu, J.-D. Grunwaldt, *Top. Catal.* **2016**, *59*, 866-874.

[51] S. Stoll, A. Schweiger, *J. Magn. Reson.* **2006**, *178*, 42–55.

FULL PAPER

By alternating between *operando* selective catalytic reduction (SCR) of NO with NH_3 conditions and NO + NH_3 flow, electron paramagnetic resonance (EPR) spectroscopy absorption spectra reveal the presence of significant amounts of oxidovanadium(IV), VO^{2+} under *operando SCR* of V_2O_5/TiO_2 and $V_2O_5/WO_3/TiO_2$ catalysts.

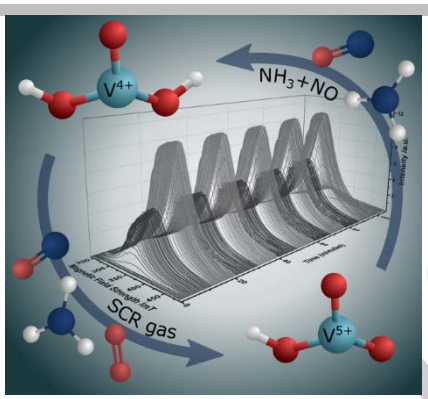

Anita L. Godiksen, Marie H. Funk, Søren B. Rasmussen, Susanne Mossin**

Page No. – Page No.

Assessing the Importance of V(IV) During NH_3-SCR Using *Operando* EPR Spectroscopy